Molecular-dynamics study of the viscous to inertial crossover in nanodroplet coalescence

Jean-Christophe Pothier and Laurent J. Lewis*

Département de Physique and Regroupement Québécois sur les Matériaux de Pointe, Université de Montréal, Case Postale 6128, Succursale Centre-Ville, Montréal, Québec, Canada H3C 3J7

(Received 17 June 2011; published 29 March 2012)

We have studied the coalescence of three-dimensional (3D), quasi-two-dimensional (quasi-2D), and 2D liquid, equal-size Cu and Si nanodroplets in the viscous and inertial regimes using classical molecular-dynamics simulations. At the onset of coalescence, a bridge (of radius r) between the droplets forms and develops until the merge is complete. For the 3D and quasi-2D systems, our results show a transition from a viscous-dominated regime at very short time, where $r \propto \tau^1$, to a regime dominated by inertial forces at longer time, with $r \propto \tau^{0.5}$, in agreement with theoretical models; the viscous regime is not observed in two dimensions, where only inertial forces seem to be operating. A detailed analysis of the 3D data suggests that the viscous-to-inertial crossover length $l_c(R_0, T)$ (with R_0 being the initial radius of the droplets and T being the temperature) behaves differently in the two systems. While $l_c \propto R_0^{1/2}$ and depends only weakly on temperature in l-Cu, as theory predicts, $l_c \propto R_0^{0.96} T^{0.41}$ in l-Si. We conclude from these observations and corresponding experimental data that the prefactor for the dependence of r on time in the inertial regime is not "universal" and actually depends on system properties, including initial radius, viscosity, and surface tension.

DOI: 10.1103/PhysRevB.85.115447 PACS number(s): 47.55.df, 68.03.−g

I. INTRODUCTION

The process of droplet coalescence is of paramount importance in many industrial applications, such as ink-jet printing, coating technologies, mixing and transportation of liquids in microfluidic devices, etc.[1–6] It can be observed in nature, in raindrop splashing and cloud drop coarsening, for instance. Because coalescence is normally triggered by the rupture of two neighboring droplets and the subsequent formation of a bridge,[7] the deformation process offers interesting opportunities for studying the droplet rupture mechanism. In the case of low-viscosity and/or nanoscale droplets, the tools presently available, however, do not permit a direct observation of the sequence of events starting with the initial rupture of the droplets to full coalescence, so that most of our current understanding in this case is based on indirect measurements or theory.[8–12]

There is ample room for further investigations therefore, and computer models, in particular, classical molecular-dynamics (MD) simulations, provide an interesting and powerful avenue for this purpose. That being said, there have been only very few studies of liquid coalescence using classical MD,[13–16] which possesses the immense advantage of being able to deal with realistic models at a reasonable computational cost (as opposed to, e.g., *ab initio* approaches). Classical MD simulations are based on, and entirely determined by, empirical or semiempirical potentials, which can be as realistic as desired (at some cost, however). In contrast, simulations based on continuous or hydrodynamic approaches require several system properties as input (viscosity, density, surface tension, etc.), and while capable of dealing with large-scale systems, these approaches provide no information on processes at the atomic scale, which is needed for studying the very early moments of coalescence of nanoscale droplets.

In the present work, using MD simulations with empirical, but realistic, interatomic potentials, we examine the coalescence (in particular its early moments) of low-viscosity liquid nanodroplets in different geometries and verify, which is our principal objective, whether or not these yield the expected transition[17] between viscous-driven and inertial-driven regimes. Our work also provides insights on how droplets evolve immediately after the rupture which signals the onset of coalescence, a stage not accessible to experiment. Indeed, nanoscale droplets are becoming increasingly relevant to various applications in nanoelectronics, and precise control of the size and structure of the droplets is required;[18] it has been shown that the morphology and size of nanoscale aggregates can be controlled by modifying either the characteristic coalescence time or the characteristic collision time, that is, the time between collision events,[19] and more importantly whether coalescence is complete before another collision takes place. Hence, a detailed understanding of the early coalescence regime is of utmost importance.

We are concerned here with two systems of interest for applications and which have different "chemistries," viz., Cu and Si: sub-10-nm Si nanoparticles are interesting for their luminescence properties,[20,21] while Cu nanoclusters are used, e.g., in self-assembled systems or in iron-based alloys to alter their properties.[22,23] That being said, our study focuses on fundamental processes so that these systems may be viewed as prototypical. A "generic" model such as Lennard-Jones could also be relevant and was in fact considered but lacks the cohesion and stability of more realistic models (mainly due to the absence of many-body contributions), a significant drawback for the study of finite-liquid clusters.

A widely accepted model for liquid coalescence has been proposed by Eggers *et al.*[24] and Duchemin *et al.*[17] According to this model, the evolution of the coalescence bridge proceeds in two steps, driven respectively by viscous and inertial forces. In the inertial regime, the radius of the bridge evolves as $r \propto \tau^{1/2}$, where τ is the time measured from the moment at which the rupture of the droplets takes place;[17] this is valid when r is larger than the viscous length l_v of the liquid

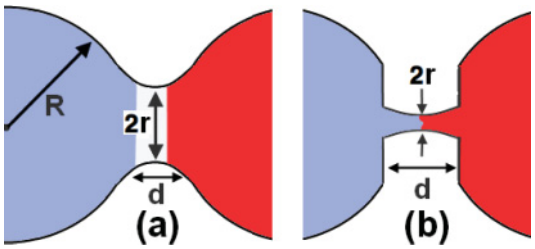

FIG. 1. (Color online) (a) Normal coalescence, with $d = r^2/R_0$, where d is the distance between the two droplets at distance r (neck radius) from the horizontal symmetry axis; (b) topological deformation in the initial linear bridge formation with $d = d_0$, with d_0 being the initial distance between the droplets.

droplets, which, for low-viscosity liquids, is always true for late stages of coalescence since r increases with time. The inertia-driven behavior has been unambiguously established both experimentally and computationally.[12,25,26]

At very early times, now, when the droplets are essentially still, the onset of coalescence results from overcoming the surface tension, and therefore, viscous forces are expected to be the main driving factor. Hopper has developed an exact solution for two-dimensional (2D) systems[27] that has been shown to apply to three-dimensional (3D) systems as well[24] provided that the distance between the droplets $d \ll r$. Here, the scaling law is of the form $r \propto \tau^a$, where a is close to unity. This model should hold irrespective of liquid viscosity as long as $r < l_v$. Since l_v is very small for low-viscosity fluids (e.g., $\sim$10 nm for water), the viscous behavior is practically unobservable by direct means; recent experiments using electrical currents to monitor coalescence are consistent with the Hopper formula, but the hypothesis underlying the interpretation of the experimental data, in particular with regard to the initial deformation of the droplets, remains to be verified.[10,12,28]

Indeed, it is not clear at present how the rupture that opens the way to coalescence proceeds, in particular whether it obeys the "normal" behavior, which follows from the assumption that the tips of the droplets remain quadratic as they evolve, as illustrated in Fig. 1(a), i.e., $d \propto r^2$, or if, rather, they are slightly flattened with the distance between them remaining roughly constant, $d = d_0$, as illustrated in Fig. 1(b).[10–12,24] In any case, at long enough times (typically microseconds for millimeter-size drops), the square-root behavior is recovered; the point at which the transition takes place between the two regimes is usually described in terms of the characteristic lengths l_v and the Ohnesorge number Oh, which we will discuss in Sec. II.

We thus aim in the present study to assess the nature of the different regimes operating in various conditions, in particular dimensionality, droplet size, and temperature. As noted above, we have considered two different materials, copper and silicon, in three different geometries: full 3D, quasi-2D (thin disks), and real 2D. The quasi-2D systems are relevant because they correspond to a geometry often used in experiment,[12,29] viz., thin, liquid, lens-shaped droplets with aspect ratio $\leqslant 10^{-3}$. The 2D systems, for their part, are expected to be equivalent to 3D systems according to Eggers *et al.*;[24] this makes them evidently interesting because they are easily amenable to very large-scale simulations (as also are quasi-2D models), a non-negligible advantage.

Anticipating our results, we find both the 3D and quasi-2D systems to exhibit a transition from an $r \propto \tau$ behavior (viscous) to an $r \propto \tau^{0.5}$ behavior (inertial), in agreement with theory. In contrast, the exact 2D system exhibits only the $r \propto \tau^{0.5}$ behavior, i.e., the initial viscous regime appears to be absent; we propose an explanation for this observation in terms of coordination and cohesion. We have analyzed the simulation data to understand more precisely the role of initial droplet radius, temperature, and material properties. The viscous-to-inertial transition can be characterized by a crossover length $l_c(R_o, T)$, the radius of the coalescence neck, which theory predicts to be universal. We find however that $l_c(R_0, T)$ behaves differently in the two systems: while $l_c \propto R_0^{1/2}$ and depends only weakly on temperature in l-Cu, as theory predicts, $l_c \propto R_0^{0.96} T^{0.41}$ in l-Si. These observations suggest that the prefactor for the dependence of r on time is in fact not "universal" but actually depends on system properties, in particular initial radius, viscosity, and surface tension.

II. THEORETICAL CONSIDERATIONS

The onset of coalescence is signaled by the rupture of the surfaces of the droplets and the formation of a bridge, of radius r, that rapidly fills the distance d between the drops as they merge (Fig. 1). For low-viscosity fluids, the coalescence process is largely driven by inertial forces; a scaling law follows from equating the capillary forces to the inertial forces:[24]

$$\frac{R_0 \sigma}{r^2} \propto \rho \left(\frac{dr}{dt}\right)^2, \tag{1}$$

where σ is the surface tension, ρ is the density of the liquid, and R_0 is the initial radius of the drops (assumed to be of equal size). Solving Eq. (1) we obtain the dependence on time of the radius of the bridge:

$$r = c \left(\frac{\sigma R_0}{\rho_0}\right)^{1/4} (t - t_0)^{1/2} = c \left(\frac{\sigma R_0}{\rho_0}\right)^{1/4} \tau^{1/2}, \tag{2}$$

with t_0 being the time at which rupture takes place (and $t - t_0 \equiv \tau$) and c being a constant of the order of unity.[9,10,17,24] This scaling law assumes that the bridge radius is larger than the viscous length of the liquid, $r > l_v = \eta^2/(\rho\sigma)$; we return to this point later in this section.

As noted earlier, irrespective of liquid viscosity, a linear dependence of r on τ is expected if $r < l_v$ and $d \ll r$ as viscous forces dominate the flow of liquid matter at very early moments of coalescence.[24,27] For drops immersed in an inviscid environment (i.e., where viscous forces from the environment are negligible), we have[24,27]

$$r = c'' \frac{\sigma}{\eta} \tau, \tag{3}$$

where η is the viscosity of the liquid droplets and (asymptotically) $c'' = -\frac{1}{\pi} \ln(\frac{\sigma\tau}{R_0\eta})$. Experiment suggests that the logarithmic dependence on time is weak[9,12,28] at best, i.e., r depends linearly on τ, with c'' being a constant of order unity; evidently, the actual state of affairs would depend on the range

of values of τ covered by the experiment as well as the initial radius R_0.

Solving Eqs. (2) and (3) for τ yields the characteristic bridge radius (crossover length) between the two regimes (viscous and inertial):

$$l_c = \eta \left(\frac{c^2}{c''}\right) \sqrt{R_0/(\sigma\rho_0)}, \tag{4}$$

where c'' would be calculated at the crossover time $\tau = \tau_c$. For low-viscosity liquids, viscous forces operate on very short time scales, and coalescence rapidly crosses over to a state which is dominated by inertial forces, as described by Eq. (2).

A linear regime may also be shown to derive from considering that the local deformations of the droplets near the coalescence bridge are nonquadratic. Indeed, Case and Nagel have shown that a linear behavior emerges if one assumes that the droplets are slightly flat when coalescence begins, as illustrated in Fig. 1(b), so that d is essentially constant ($=d_0$).[10,11] With this new geometry and given the relation between the length of the bridge and its radius, $d = r^2/R_0$ (see Ref. 24), Eq. (1) becomes[10,11]

$$\frac{\sigma}{d_0} \propto \rho \left(\frac{dr}{dt}\right)^2, \tag{5}$$

yielding

$$r = c' \left(\frac{\sigma}{\rho d_0}\right)^{1/2} \tau. \tag{6}$$

Solving Eqs. (2) and (6) for τ yields the characteristic bridge radius (crossover length) between the two regimes:

$$l_c = \frac{c^2}{c'} \sqrt{R_0 d_0}. \tag{7}$$

In this model, the transition between the two regimes is related to topological features of the deformation. Thus, Eq. (6) dominates the flow until the flattening disappears and the normal inertial behavior, Eq. (2), takes over.

The above formalism assumes that the fluids have low viscosity, e.g., water, for which $\eta \sim 1$ mPa s.[24] The systems we investigate here, l-Si and l-Cu, have viscosities in the range 0.37–0.6 mPa s (Refs. 30–33) and 1.5–2.4 mPa s (Refs. 34 and 35), respectively, depending on temperature, which can also be considered as "low." This can in fact be assessed more precisely by considering the Ohnesorge numbers and the viscous lengths of the fluids.

The Ohnesorge number, given by $Oh = \eta/\sqrt{\rho\sigma R_0}$, relates the viscous forces to the surface tension and inertial forces. A low value of Oh indicates a lesser influence of viscosity.[36,37] When $Oh > 1$, viscous forces dominate and retard the process; in contrast, when $Oh < 1$, inertial forces dominate.[36] For l-Cu, $Oh \sim 0.1$–0.3 (vs $\sim$0.001 for millimeter-size water droplets), while $Oh \sim 0.07$–0.15 for l-Si; note that the surface tension σ varies with temperature.[31,38] Thus, both our systems should be inertia dominated, and Eq. (2) should apply. However, because the Oh values of our systems are relatively close to the "critical" value (1), we expect a significant influence of viscous forces, especially early in the coalescence process when the drops are completely still.

Also, in order to determine the relative importance of viscous forces, the viscous length $l_v = \eta^2/(\rho\sigma)$ may be compared to the bridge radius r: when $r > l_v$, the inviscid theory would apply. Here we have $l_v \sim 0.7$–1.7 Å and $l_v \sim 3.2$–6.5 Å for l-Si and l-Cu, respectively. Thus, again, both our systems are close to the viscous-inertial crossover point: $l_v \sim r$ early in the coalescence process, but as time proceeds, r will surpass l_v, so that the scaling law predictions of Eq. (2) apply.

III. COMPUTATIONAL DETAILS

As mentioned above, we considered two different materials in order to assess the universal character of the coalescence process and the relevant models, viz., l-Cu and l-Si. For l-Cu, we studied the problem in three different geometries: 3D, quasi-2D, and 2D; in all cases, the embedded-atom method (EAM) potential has been used,

$$E_i = F_\alpha \left[\sum_{j\neq i} \rho_\alpha(r_{ij})\right] + \frac{1}{2}\sum_{j\neq i} \phi_{\alpha\beta}(r_{ij}), \tag{8}$$

with parameters appropriate to each configuration (2D, Refs. 39 and 40; quasi-2D and 3D, Ref. 41); the cutoff was set to 5 Å. The radius of the 2D nanodroplets ranged between 30 and 100 nm, and temperature was varied between 1700 and 2000 K; the latter are high enough for coalescence to proceed swiftly, but low enough that evaporation is not a significant problem. In quasi-2D and 3D geometries, the radius of the droplets was in the range 5–35 nm, and temperatures were in the range 1700–2500 K; note that $T_{\rm melt} \sim 1320$ K in 2D and $\sim$1380 K in 3D (both EAM) and $T_{\rm boil} = 2835$ K (experiment; cf. Refs. 40,42 and 43). The systems we study here are nanometer size but nevertheless satisfy the $d \ll r$ condition (except at very early moments of coalescence), at least early enough in the coalescence process, so that viscous forces should be meaningful.

For l-Si, the Stillinger-Weber (SW) potential,[44,45] cutoff at 4 Å, was employed:

$$E = \sum_i \sum_{j\neq i} \phi_2(r_{ij}) + \sum_i \sum_{j\neq i} \sum_{k>j} \phi_3(r_{ij}, r_{ik}, \Theta_{ijk}), \tag{9}$$

where ϕ_2 and ϕ_3 represent two-body and three-body interactions, respectively. Here the droplets varied in radius between 7 and 12 nm, and temperature varied between 1800 and 2500 K vs $T_{\rm melt} = 1691$ K (SW) and $T_{\rm boil} = 3538K$ (experiment).[46]

Prior to simulating the coalescence process, the nanodroplets were prepared individually by melting, thermalizing, and stabilizing spheres (3D), thin disks (quasi-2D), or disks (2D) of material. We verified that the densities, radial distribution functions, and diffusion coefficients were consistent with values from the literature.[47–52] The droplets were then placed in near contact to one another, i.e., at a distance $\sim$3–4 Å, slightly shorter than the interaction range of the potentials. No initial velocities were given to the droplets so that coalescence is purely energy driven. The center-of-mass motion was subtracted when necessary, which was seldom the case. Thermalization was interrupted during coalescence (and temperatures remained constant to within a few tens of

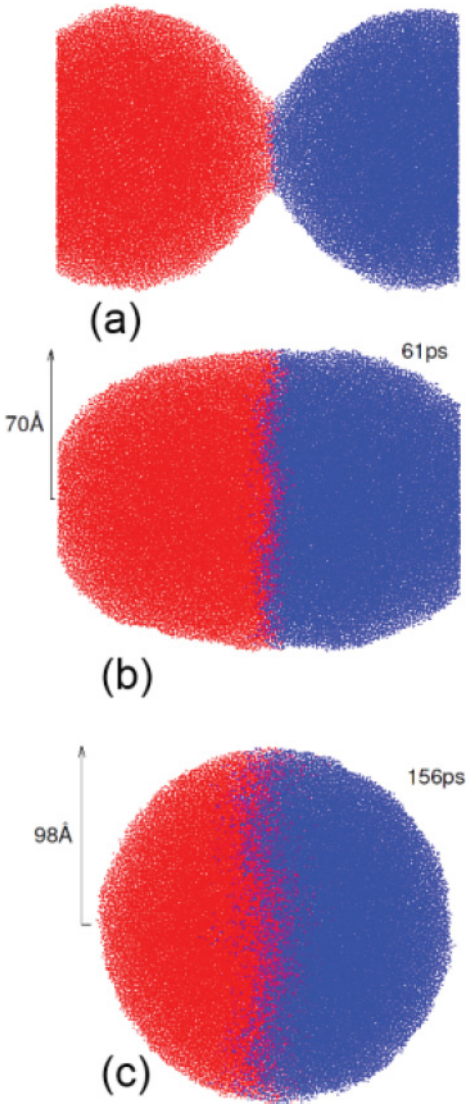

FIG. 2. (Color online) Coalescence of two *l*-Si nanodroplets as a function of time: (a) early in the coalescence process, (b) when $r = R_0$, and (c) at complete coalescence. The initial radius of the droplets is 77 Å, and the temperature is ∼1800 K. The atoms are colored according to the nanodroplet to which they belong.

degrees at the highest temperatures). For the particular case of quasi-2D droplets, which consist of disks of finite thickness (8.5–13.5 Å), periodic boundary conditions in the z direction (perpendicular to the plane of the droplets) are imposed during the relaxation stage; these are removed during coalescence, and the geometry is maintained by forcing the z component of all velocities and forces to zero, so that the system cannot deform to a sphere, as it would tend to do.

All calculations were carried out using our own computer programs as well as the package LAMMPS, an excellent open-source multiprocessor classical MD code.[53] The coalescence simulations were performed in the microcanonical ensemble using time steps in the range 0.3–0.7 fs, depending on temperature. Following each simulation, the average bridge radius was determined using a surface-finding algorithm, as discussed in the Appendix. Also, most simulations were repeated several times in order to improve statistics; overall,

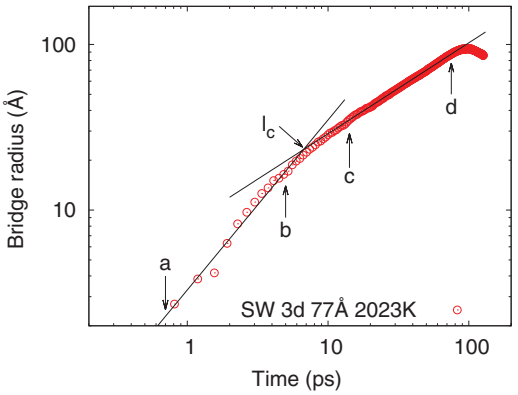

FIG. 3. (Color online) Bridge radius as a function of time for 77-Å *l*-Si droplets at 2000 K.

we examined 25 systems in 2D, 4 systems in quasi-2D, and 27 systems in 3D. By way of illustration, we present in Fig. 2 three snapshots of the coalescence of *l*-Si nanodroplets with initial radius $R_0 = 77$ Å and temperature ∼1800 K.

IV. RESULTS

A. Power-law regimes

1. 3D models

We discuss first the dependence of the bridge radius on time in order to assess the existence of the two power-law regimes and the crossover between them. An example of this is presented in Fig. 3 for the coalescence of two *l*-Si droplets of initial size 77 Å at temperature $T \sim 2000$ K. The two regimes, viscous and inertial, are clearly visible; they are fitted to power laws [$\log(r) = \alpha * \log(\tau) + e$, where r is the radius of the coalescence neck, τ is the time of coalescence, α is the exponent of the power law, and e is an adjustment constant] within the limits indicated (a to b for the viscous regime and c to d for the inertial regime); also indicated is the crossover length l_c. Likewise, we show in Fig. 4 corresponding results for *l*-Cu nanodroplets of different sizes and at different temperatures.

The 3D systems we examined all display the two-regime behavior. The various parameters characterizing the two

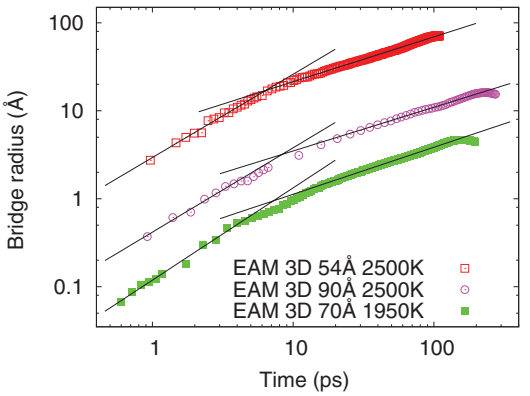

FIG. 4. (Color online) Bridge radius as a function of time for different *l*-Cu droplets, as indicated; the 90- and 70-Å curves have been shifted down for clarity.

TABLE I. Parameters characterizing coalescence, exponents of the power laws in the viscous (α_{Viscous}) and inertial (α_{Inertial}) regimes as well as crossover lengths l_c, for the l-Cu droplets at the initial radii and temperatures indicated. The number in parentheses is the error bar on the last digit.

R_0 (Å)	T (K)	α_{Viscous}	α_{Inertial}	l_c (A)
52	2024	0.92(4)	0.508(2)	30
54	2523	0.95(2)	0.510(2)	34
67	1815	0.64(2)	0.526(1)	35
67	2015	0.95(2)	0.534(1)	46
68	1726	0.93(2)	0.526(1)	33
70	1766	1.36(9)	0.530(1)	41
70	1864	0.83(3)	0.537(1)	37
70	1964	1.05(3)	0.534(1)	38
70	2118	1.14(7)	0.548(1)	38
70	2219	1.02(2)	0.553(1)	42
70	2311	0.77(8)	0.526(1)	24
70	2496	0.67(2)	0.526(2)	38
80	2514	1.03(5)	0.506(3)	51
90	2515	0.96(4)	0.497(7)	48
111	2504	0.77(5)	0.462(4)	54

regimes (viscous and inertial exponents and crossover length) are presented in Tables I and II. To summarize these results, the power-law exponents for the viscous and inertial regimes average to 0.9 ± 0.2 and 0.52 ± 0.02 for l-Cu droplets and 1.00 ± 0.08 and 0.53 ± 0.03 for l-Si droplets, in agreement with both the linear and square-root behaviors discussed earlier (modulo the statistical error). Note that it has been proposed that the flattening effect may result from the presence of a fluid (e.g., air or surfactant) in which the droplets are lying in real experiments;[11] our simulations seem to rule out this possibility since the droplets are in vacuum. Hence, the existence of two regimes would be inherent to the coalescence process. As for the crossover length, it will be discussed in Sec. IV C.

2. 2D models

We proceed now with a corresponding study for the 2D l-Cu models. Typical results for the variation in time of the bridge radius are presented in Fig. 5 and summarized in Table III. While we do consistently observe the inertial regime, with an

TABLE II. Same as Table I for the l-Si droplets.

R_0 (Å)	T (K)	α_{Viscous}	α_{Inertial}	l_c (Å)
77	1796	1.06(4)	0.574(1)	48
77	1926	0.95(3)	0.552(1)	51
77	2023	1.03(3)	0.549(1)	46
77	2125	1.07(3)	0.526(1)	46
77	2215	0.97(3)	0.5201(6)	43
77	2327	0.92(4)	0.548(1)	50
77	2423	1.05(3)	0.556(1)	44
77	2525	0.93(5)	0.501(1)	58
80	2530	1.13(4)	0.545(5)	52
90	2518	0.83(7)	0.496(2)	71
121	2510	1.02(9)	0.483(3)	78

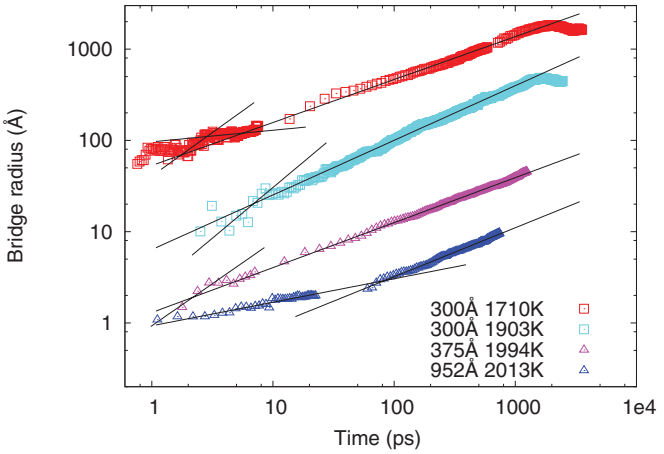

FIG. 5. (Color online) Bridge radius as a function of time for l-Cu 2D droplets. For clarity the results have been shifted up and down (except those for 300-Å, 1900 K droplets).

average exponent of 0.55 ± 0.04, i.e., close to the predicted value of 0.5, the linear viscous regime is, at best, ill defined. As can be seen in Table III and Fig. 5, the viscous-inertial transition is seldom observed, and the viscous power-law is certainly not linear. In addition, the crossover lengths that we can reasonably extract from the data are in complete disagreement with the values predicted on the basis of Eqs. (4) and (7); the latter were deduced from quasi-2D and 3D simulations to serve as reference, recalling that, according to Ref. 24, l_c is independent of dimensionality. The crossover length is discussed in more detail in Sec. IV C.

The above results can be explained, to some degree, by considering the differences in the coordination numbers and binding energies between 2D and 3D systems. The viscous regime is, by definition, dominated by viscous forces as these oppose resistance to the deformation of the droplets. If the binding energy and average coordination are "small," the overall resistance to deformation is reduced, thus promoting an inertia-driven mechanism. This is the situation for 2D systems; as indicated in Table IV, the average coordination

TABLE III. Power-law exponents for the two regimes as well as measured and calculated crossover lengths for the coalescence of 2D l-Cu droplets. For l_c, the measured value is obtained by fitting to the data, while the calculated value is obtained by fitting to Eqs. (4) and (7).

R_0 (Å)	T (K)	α_{Viscous}	α_{Inertial}	l_c (Å) Meas.	l_c (Å) Calc.
300	1710		0.487(4)		44
300	1903	1.2(2)	0.598(1)	20	44
300	2001	1.1(1)	0.536(1)	35	44
375	1994	0.9(2)	0.500(1)	19	50
430	1994		0.511(2)		54
491	1884	0.92(8)	0.575(2)	67	58
492	1799	0.8(1)	0.498(1)	48	58
493	1720	0.61(6)	0.556(2)	77	58
496	1992	0.90(5)	0.611(4)	30	58
952	2013	0.26(1)	0.554(2)	145	84
960	1724	0.42(2)	0.599(1)	51	84

TABLE IV. Coordination and binding energy for 2D and 3D *l*-Cu at $T \sim 2000$ K.

Dimension	Average coordination	Binding energy (eV)
2D	5.8	2.3
3D	12	3.0

and binding energy of the 2D systems are much smaller than for the 3D systems. It appears, in fact, that 2D systems are relatively unstable in the period during which the bridge starts to form (because viscous forces are too weak) and rapidly move to inertia-dominated dynamics after the bridge forms.

To ascertain this explanation, we undertook to examine quasi-2D systems, for which the topological limitations on coordination and binding energy should be largely removed and which, it so happens, correspond more closely to the real "lens geometry" used in experiment. We discuss this next.

3. *Quasi-2D models*

We present in Table V and Fig. 6 the results for the quasi-2D systems. As could be expected from the discussion above, we observe in all cases a well-defined transition from viscous-dominated to inertial-dominated coalescence, with corresponding exponents of 1.0 ± 0.1 and 0.54 ± 0.04, in close agreement with the predictions of the linear and quadratic models, respectively. Thus, true 2D systems appear not to exhibit the viscous-force-dominated regime, and in effect, a thin, but finite, extra dimension seems to be required for it to emerge; this is certainly the case for nanoscale droplets, where the definition of viscosity or viscous forces becomes problematic.

B. Dependence on temperature and initial radius

We examine in more detail here the effect of temperature and initial radius on the coalescence process. In the inertial regime, Eq. (2) can be rewritten by introducing the characteristic inertial time,[26] $\tau_i = \sqrt{\rho R_0^3/\sigma}$, as follows:

$$r/R_0 = c(\tau/\tau_i)^{0.5}; \tag{10}$$

τ_i must be calculated for each system since it depends on droplet size and temperature. For the *l*-Cu droplets, τ_i varies between 35 ps for 52-Å droplets and 558 ps for 360-Å droplets. For *l*-Si droplets τ_i is consistently smaller at equivalent radius, e.g., $\tau_i^{\mathrm{Si}} = 40$ ps for an 80-Å droplet at 2500 K, while $\tau_i^{\mathrm{Cu}} = 59$ ps.

TABLE V. Same as Table I for the quasi-2D *l*-Cu droplets.

R_0 (Å)	T (K)	$\alpha_{\mathrm{Viscous}}$	$\alpha_{\mathrm{Inertial}}$	l_c (A)
335	2201	0.88(5)	0.539(4)	87
350	2518	1.16(3)	0.485(5)	107
354	2406	0.93(3)	0.550(3)	109
360	2323	1.03(3)	0.588(2)	93

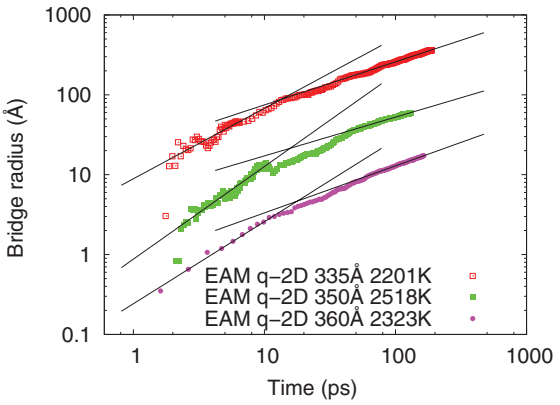

FIG. 6. (Color online) Bridge radius as a function of time for the quasi-2D droplets. The 350- and 360-Å curves have been shifted down for clarity.

We present in Fig. 7(a) our results for the radius of the coalescence bridge as a function of time for the *l*-Cu droplet simulations reported in Table I; Fig. 7(b) shows the same data after rescaling the time by τ_i and the radius by R_0. The different curves now collapse onto a single one whose slope is $\sim 0.84 \pm 0.09$, corresponding to the value of c in Eq. (10). The exact value of this constant is not known: as indicated in Table VI,

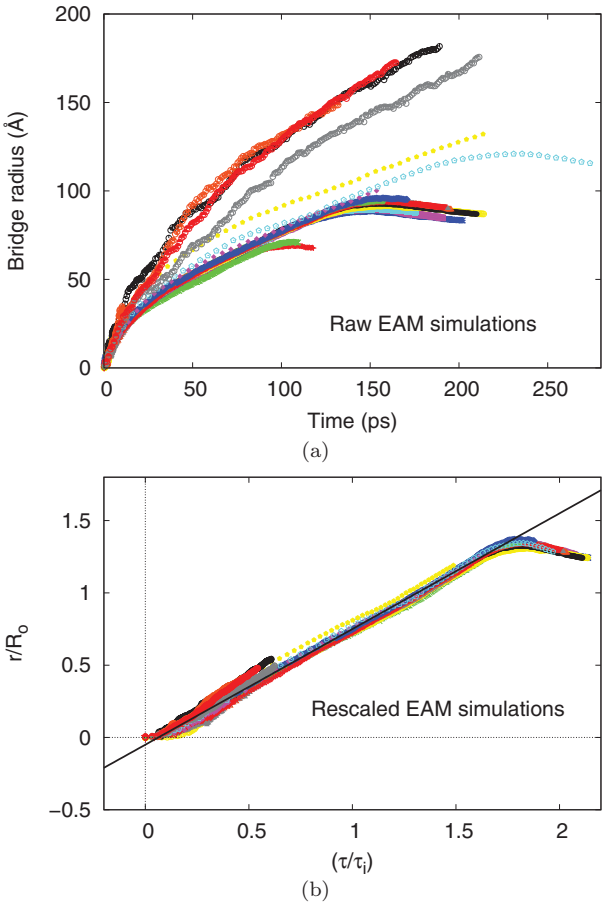

FIG. 7. (Color online) (a) Bridge radius vs time for the *l*-Cu simulations. (b) Same data collapsed, i.e., time rescaled by τ_i and radius rescaled by R_0.

TABLE VI. Numerical and experimental values of constant c in Eq. (2). Also indicated are the surface tension σ and the viscosity η, as well as the maximum size ratio r/R_0 investigated. The asterisks (*) indicate experimental measurements.

Liquid type	r/R_0 (max)	σ (mN/m)	η (mPas)	c
Numerical[17]	0.035			1.62
Methanol*[26]	0.5	22	0.59	1.29(5)
Silicon oil*[9]	0.5	20	5	1.24
Water*[9]	0.5	72	1	1.14
Silicon oil*[9]	0.5	20	20	1.11
Water*[26]	0.5	72	1	1.09(8)
Water/glycerin*[26]	0.5	67.4	14.1	1.03(7)
l-Cu (this work)	1.1	∼1000	∼2	0.84(9)
l-Si (this work)	1.1	∼800	∼0.5	0.91(5)

some experiments indicate that it lies in the range 1.03–1.29 (Refs. 9 and 26), while the numerical calculations of Duchemin *et al.* (using a boundary integral method) suggest $c = 1.62$ irrespective of liquid.[17] The latter appears to be inconsistent with the values from both experiment and the present work. One obvious difference is the size regime investigated, given in Table I, much smaller in Duchemin *et al.* In any case, $c \sim 1$ and the exact value evidently depends on the type of material, as can be inferred from Table VI. This is indeed what we find: $c_{\rm fit} = 0.84 \pm 0.09$ for l-Cu and $c = 0.91 \pm 0.05$ for l-Si; we note in passing that larger values of σ seem to be correlated with smaller c, as observed here.

The situation is far less clear for l-Si, as can be appreciated from Fig. 8. The rescaling, shown in Fig. 8(b), is not at all perfect; we note in particular that the deviations are more pronounced for droplets with larger initial radius and temperature, which evolve supralinearly, i.e., faster than for smaller and colder droplets. In order to improve, or rather assess, the universal character of the data, we introduced a different characteristic inertial "variable" $\tau_{i2} = \tau_i C$, where $C = \sqrt{R_0^a T^b}$, and varied a and b so as to minimize the deviation in the r/R_0 axis. The best solution was found when $a = -1.24$ and $b = -0.77$. The results are displayed in Fig. 8(c). [In order to check our procedure, we have performed a corresponding calculation for Cu and found $a = 0$ and $b \sim -0.2$, which yields a temperature dependence $T^{0.05}$, clearly negligible (and within error) for the temperature range considered here; this result is consistent with the almost-perfect fit of Fig. 7(b).]

There could be several explanations for the fact that the l-Si data do not follow the expected behavior. One possibility is that the coalescence process, especially on such short length scales, is more sensitive to the physical properties and the initial topology of the droplets than assumed in the theoretical models. With this in mind, we can substitute τ_{i2} in Eq. (10) and expand to yield the following expression for the scaling law:

$$r_{\rm Si} \sim c \left(\frac{R_0\sigma}{\rho}\right)^{1/4} \tau^{1/2}\left(R_0^{0.3} T^{0.2}\right). \qquad (11)$$

While this operation is somewhat *ad hoc*, it does demonstrate that materials are not all born equal; i.e., the scaling law does depend on the specifics of the material. In particular, here, we see (and this is coherent with our observations pertaining to Table VI) that l-Si droplets are more sensitive to initial physical parameters, notably R_0, as well as temperature. Thus, the constant c, far from being universal, is material and temperature dependent, viz., $c = c(R,T,\sigma,\eta)$. To pursue this, we have found that the values of the constants in Table VI could be well described by the *ad hoc* formula $c = 2/(\sigma^{0.13}\eta^{0.06})$, as demonstrated in Table VII, showing that this parameter is indeed not constant. Evidently, the fit is empirical but does demonstrate the sensitivity of c to material properties, and the same logic applies to both simulations and experiments, so that these conclusions are not an artifact of the model.

C. Crossover length

The crossover length l_c is a clear expression of the passage from the viscous regime to the inertial regime. This can be extracted from the coalescence data presented above or calculated using Eqs. (4) or (7), which both state that $l_c \propto \sqrt{R_0}$, with R_0 being the initial radius of the droplets. We present in Fig. 9 a plot of the simulated l_c as a function of R_0 for both l-Cu and l-Si droplets. For l-Cu, a fit to the MD data yields an exponent of 0.57 ± 0.04, which is consistent with the models presented above. The value of the slope, the constant in $l_c = {\rm const} R_0^{0.57}$, is 8.25×10^{-5}. This can be used to establish the connection with the models summarized in Eqs. (4) and (7), namely, const $= \eta(\frac{c^2}{c''})\sqrt{1/(\sigma\rho_0)}$ for the normal behavior and const $= \frac{c^2}{c'}\sqrt{d_0}$ for the flattening model; recall that $c = 0.84$.

TABLE VII. Numerical and experimental values of c (cf. Table VI) compared to fitted values $c_{\rm fit} = 2/(\sigma^{0.13}\eta^{0.06})$ (see text).

Liquid type	c	$c_{\rm fit}$
Methanol[26]	1.29(5)	1.38
Silicon oil[9]	1.24	1.23
Water[9]	1.14	1.15
Silicon oil[9]	1.11	1.13
Water[26]	1.09(8)	1.15
Water/glycerin[26]	1.03(7)	0.98
l-Cu (this work)	0.84(9)	0.78
l-Si (this work)	0.91(5)	0.88

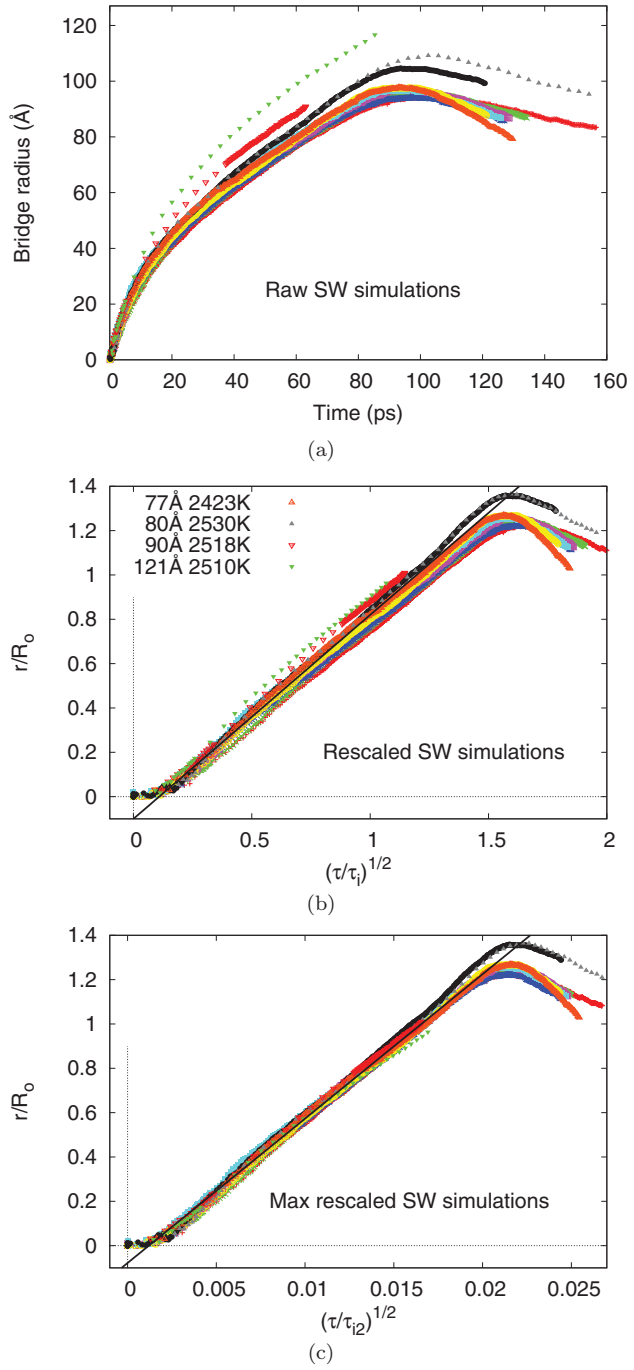

FIG. 8. (Color online) (a) Bridge radius vs time for the l-Si simulations. (b) Same data collapsed, i.e., time rescaled by τ_i and radius rescaled by R_0; the slope of the black line is 0.91. (c) Same data maximally collapsed; see text for details.

For the flattening model we find $c'_{\mathrm{Cu}} = 0.17$, somewhat smaller than the value given by Case and Nagel, $c' \approx 1$ (Ref. 10). For the normal behavior, now we have $c''_{\mathrm{Cu}} = 0.15$–0.22 [averaged to 0.18(2)]. This can be compared to the corresponding value of $c'' = -\frac{1}{\pi}\ln(\frac{\sigma\tau}{R_0\eta})$ from Eq. (3) at the simulated crossover time, $\tau = \tau_c$, viz., $c'' = 0.12$–0.45 (average at 0.22 ± 0.12), remarkably close to the values from our simulations. We conclude from this that l-Cu follows the normal behavior of early coalescence rather than the flattening

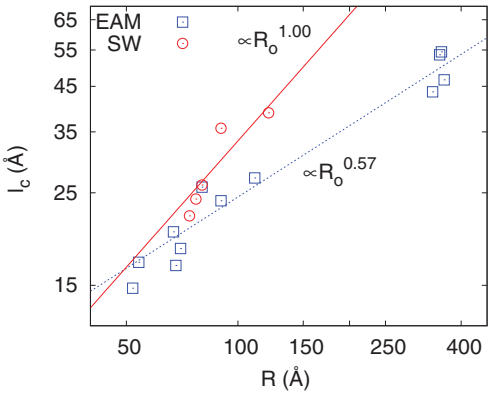

FIG. 9. (Color online) Crossover length as a function of initial droplet radius for the 3D l-Cu and l-Si models.

behavior. Also, our results indicate that the logarithmic term in c'' is significant [cf. Eq. (3)], and neglecting it (so that $c'' \approx 1$) is probably not warranted,[9,12,28] at least at τ_c, noting, however, that the argument evidently depends on the ratio τ/R_0.

A corresponding calculation for l-Si yields $l_c \propto R_0^a$, with $a = 1.0 \pm 0.3$, larger than the value of 0.5 provided by the models discussed earlier [Eqs. (4) and (7)], but expected in view of the "unusual" dependence of r_{Si} found above, Eq. (11). Using the latter equation together with Eqs. (3) and (6) for the viscous regime, we obtain a crossover length of the form (the same for normal and flattening models)

$$l_c = \mathrm{const} R_0^{1.1} T^{0.4}. \tag{12}$$

This prediction can be assessed by fitting the numerical l_c data for l-Si to $\mathrm{const} R_0^a T^b$, which yields $a = 0.96$ and $b = 0.41$, in remarkable agreement with the values of Eq. (12), thus providing evidence for its validity; i.e., l-Si does not obey the usual $R_0^{0.5} T^0 = R_0^{0.5}$ dependence. However, the agreement of the numerical data with the predictions of Eqs. (4) and (7) indicates that the viscous regime is normal, provided that r_{Si} is described by Eq. (11). Whether the deformation is quadratic [Eq. (4)] or flattened [Eq. (7)], however, remains to be determined. We have tried to resolve this issue on the basis of the constants (c' and c'') that we could extract from the MD data, and the results are inconclusive. This may result from a limitation of the theory or a peculiarity of the potential model (SW); further investigations are necessary to resolve this point.

V. CONCLUSION

Using MD simulations, we have studied the coalescence of nanoscale liquid-silicon and liquid-copper droplets in 2D, quasi-2D, and 3D geometries. We find that the 3D and quasi-2D systems undergo a transition from a viscous regime, where the radius of the bridge $r_{\mathrm{viscous}} \propto \tau$, to an inertial regime, where $r_{\mathrm{inertial}} \propto \tau^{1/2}$, irrespective of initial droplet size and temperature. In 2D, only the inertial regime is observed; the lower coordination number and binding energies cause the droplets to be more prone to deformations, thus favoring the inertia-driven behavior.

Our results for l-Cu, viz., the time dependence of the bridge radius r and the crossover length l_c between viscous

and inertial regimes, are consistent with experiment[9,10,12,26] as well as the theory of Eggers *et al.*[24] and Duchemin *et al.*,[17] more precisely $l_c^{\mathrm{Cu}} \propto \sqrt{R_0}$. However, the prefactor affecting the time dependence of the radius in the inertial regime, $r/R_0 = c(\tau/\tau_i)^{0.5}$, is smaller than predicted by theory and in fact sensitive to specific properties of the material, i.e., not universal. Our results further suggest that the viscous regime is normal, i.e., quadratic deformations as opposed to flattened. The situation is more complex in *l*-Si, where the dependence on initial parameters is stronger; indeed, we have here $r \propto R_0^{0.55} T^{0.2}$ and $l_c \propto R_0^{0.96} T^{0.41}$, while theory predicts $r \propto R_0^{0.25}$ and $l_c \propto R_0^{0.5}$. Thus, again, these results indicate that the inertial regime constant for the evolution of the bridge radius c is material and temperature dependent, $c = c(R,T,\sigma,\eta)$.

The systems we considered, *l*-Cu and *l*-Si, may not be ideal representations of experimental situations but were chosen because they are prototypical and easily amenable to the large-scale simulations needed to investigate the problem. Irrespective of the specifics of the two materials, our results demonstrate clearly the transition from a viscous-dominated to an inertial-dominated regime. The transition is, however, not universal in the sense that the parameters describing the two regimes and the crossover between them depend to some degree on the properties and the chemistry of the materials involved.

ACKNOWLEDGMENTS

This work has been supported by grants from the Natural Sciences and Engineering Research Council of Canada (NSERC) and the Fonds Québécois de la Recherche sur la Nature et les Technologies (FQRNT). We are grateful to the Réseau Québécois de Calcul de Haute Performance (RQCHP) for generous allocations of computer resources.

APPENDIX

We present here the method we employed to calculate the bridge radius of a given configuration. As an illustration,

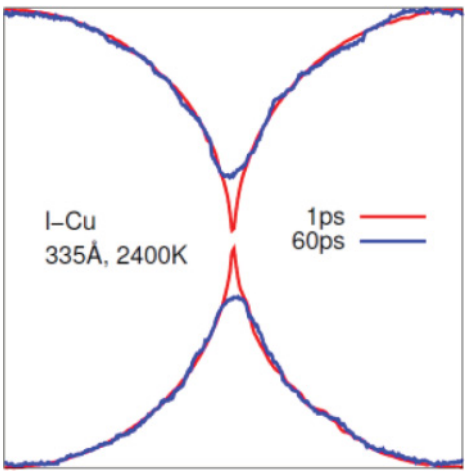

FIG. 10. (Color online) Surface of two *l*-Cu nanodroplets at 1 and 60 ps in the coalescence process.

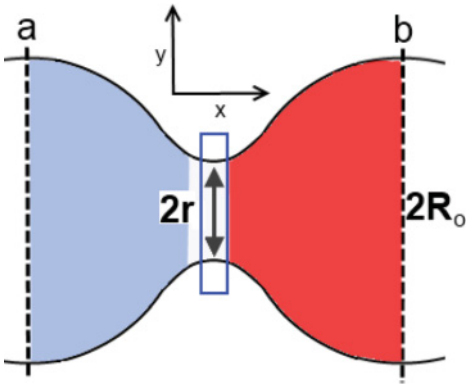

FIG. 11. (Color online) Calculation of the bridge diameter $2r$ when $r < R_0$; see text for details.

Fig. 10 shows the coalescence status of 2D *l*-Cu nanodroplets at two different times, viz., 1 and 60 ps after the onset of coalescence. For 2D systems, at each time step in the simulations, we determine the maximum width of the nanodroplets (along the coalescence axis), as indicated by points a and b in Fig. 11; initially, the width is maximum at the center of the droplets. We can "draw" the surface by moving a rectangular window along the coalescence axis between the two maxima and identifying the atoms that lie at minimum and maximum y positions; the width of the window, which is small (a few interatomic distances), is varied so as to provide better statistical accuracy as well as smooth out (or average out) the surface. The minimum distance along the y axis is the diameter of the coalescence neck, $2r$. Evidently, there will come a time at which r exceeds the initial radius; in this case, the neck radius corresponds to the maximum rather than the minimum.

For 3D nanodroplets, we use essentially the same approach, but with an additional window of width p to identify the position of the extremum of the neck, as illustrated in Fig. 12(a). Because there is no preferred direction *a priori*, the calculation is repeated for several angular directions [sweeping the full 360°; cf. Fig. 12(b)], and the radius is taken as the average of these measurements.

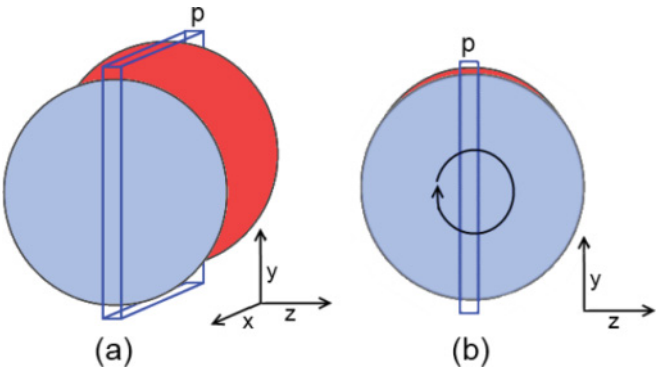

FIG. 12. (Color online) Construction for the coalescence of 3D droplets: (a) lateral view of the slab of thickness p and (b) rotation of the slab for averaging out; see text for details.

*laurent.lewis@umontreal.ca

[1] O. Reynolds, Proc. Manchester Lit. Philos. Soc. **21**, 1 (1881).
[2] L. Rayleigh, Proc. R. Soc. London **28**, 406 (1879).
[3] D. R. Reyes, D. Iossifidis, P.-A. Auroux, and A. Manz, Anal. Chem. **74**, 2623 (2002).
[4] G. F. Christopher, J. Bergstein, N. B. End, M. Poon, C. Nguyen, and S. L. Anna, Lab Chip **9**, 1102 (2009).
[5] N. Bremond, A. R. Thiam, and J. Bibette, Phys. Rev. Lett. **100**, 024501 (2008).
[6] T. Lee and P. F. Fischer, Phys. Rev. E **74**, 046709 (2006).
[7] A. Oron, S. H. Davis, and S. G. Bankoff, Rev. Mod. Phys. **69**, 931 (1997).
[8] S. Thoroddsen, T. Etoh, and K. Takehara, Annu. Rev. Fluid Mech. **40**, 257 (2008).
[9] D. G. A. L. Aarts, H. N. W. Lekkerkerker, H. Guo, G. H. Wegdam, and D. Bonn, Phys. Rev. Lett. **95**, 164503 (2005).
[10] S. C. Case and S. R. Nagel, Phys. Rev. Lett. **100**, 084503 (2008).
[11] S. C. Case, Phys. Rev. E **79**, 026307 (2009).
[12] J. C. Burton and P. Taborek, Phys. Rev. Lett. **98**, 224502 (2007).
[13] J. Koplik, S. Pal, and J. R. Banavar, Phys. Rev. E **65**, 021504 (2002).
[14] T. Hawa and M. Zachariah, J. Aerosol Sci. **37**, 1 (2006).
[15] T. Hawa and M. R. Zachariah, Phys. Rev. B **69**, 035417 (2004).
[16] L. J. Lewis, P. Jensen, and J.-L. Barrat, Phys. Rev. B **56**, 2248 (1997).
[17] L. Duchemin, J. Eggers, and C. Josserand, J. Fluid Mech. **487**, 167 (2003).
[18] J. D. Aiken and R. G. Finke, J. Mol. Catal. A Chem. **145**, 1 (1999).
[19] T. Hawa and M. R. Zachariah, Phys. Rev. B **71**, 165434 (2005).
[20] L. Patrone, D. Nelson, V. I. Safarov, S. Giorgio, M. Sentis, and W. Marine, Appl. Phys. A: Mater. Sci. & Proc. **69**, S217 (1999).
[21] L. Wang, H. Tu, S. Zhu, and J. Du, J. Phys. D **41**, 045302 (2008).
[22] M. J. Konstantinović, B. Minov, Z. Kutnjak, and M. Jagodić, Phys. Rev. B **81**, 140203 (2010).
[23] M. Fuentes-Cabrera, B. H. Rhodes, J. D. Fowlkes, A. López-Benzanilla, H. Terrones, M. L. Simpson, and P. D. Rack, Phys. Rev. E **83**, 041603 (2011).
[24] J. Eggers, J. R. Lister, and H. A. Stone, J. Fluid Mech. **401**, 293 (1999).
[25] A. Menchaca-Rocha, A. Martínez-Dávalos, R. Núñez, S. Popinet, and S. Zaleski, Phys. Rev. E **63**, 046309 (2001).
[26] M. Wu, T. Cubaud, and C. M. Ho, Phys. Fluids **16**, L51 (2004).
[27] R. W. Hopper, J. Fluid Mech. **213**, 349 (1990).
[28] J. D. Paulsen, J. C. Burton, and S. R. Nagel, Phys. Rev. Lett. **106**, 114501 (2011).
[29] H. Zeng, B. Zhao, Y. Tian, M. Tirrell, L. G. Leal, and J. N. Israelachvili, Soft Matter **3**, 88 (2007).
[30] Z. Zhou, S. Mukherjee, and W.-K. Rhim, J. Cryst. Growth **257**, 350 (2003).
[31] H. P. Wang, B. C. Luo, and B. Wei, Phys. Rev. E **78**, 041204 (2008).
[32] S. Glasstone, K. J. Laidler, and H. Eyring, *The Theory of Rate Processes: The Kinetics of Chemical Reactions, Viscosity, Diffusion and Electrochemical Phenomena* (McGraw-Hill, New York, 1941).
[33] K. Kakimoto, J. Appl. Phys. **77**, 4122 (1995).
[34] X. Han, M. Chen, and Y. Lü, Int. J. Thermophys. **29**, 1408 (2008).
[35] T. Matsumoto, H. Fujii, T. Ueda, M. Kamai, and K. Nogi, Meas. Sci. Technol. **16**, 432 (2005).
[36] H. Aryafar and H. P. Kavehpour, Phys. Rev. E **78**, 037302 (2008).
[37] H. Aryafar and H. Kavehpour, Phys. Fluids **18**, 072105 (2006).
[38] H. Fujii, T. Matsumoto, S. Izutani, S. Kiguchi, and K. Nogi, Acta Mater. **54**, 1221 (2006).
[39] M. S. Daw and M. I. Baskes, Phys. Rev. Lett. **50**, 1285 (1983).
[40] D. Belashchenko and Y. Zhuravlev, Inorg. Mater. **44**, 939 (2008).
[41] S. M. Foiles, M. I. Baskes, and M. S. Daw, Phys. Rev. B **33**, 7983 (1986).
[42] B. Sadigh and G. Grimvall, Phys. Rev. B **54**, 15742 (1996).
[43] H. Pang, Q. Pan, and P. H. Song, Phys. Rev. B **76**, 064109 (2007).
[44] F. H. Stillinger and T. A. Weber, Phys. Rev. B **31**, 5262 (1985).
[45] C. Krzeminski, Q. Brulin, V. Cuny, E. Lecat, E. Lampin, and F. Cleri, J. Appl. Phys. **101**, 123506 (2007).
[46] J. Q. Broughton and X. P. Li, Phys. Rev. B **35**, 9120 (1987).
[47] I. Štich, R. Car, and M. Parrinello, Phys. Rev. B **44**, 4262 (1991).
[48] Y. Waseda and K. Suzuki, Z. Phys. B **20**, 339 (1975).
[49] Y. Waseda, *The Structure of Non-crystalline Materials: Liquids and Amorphous Solids* (McGraw-Hill, New York, 1980).
[50] A. Pasquarello, K. Laasonen, R. Car, C. Lee, and D. Vanderbilt, Phys. Rev. Lett. **69**, 1982 (1992).
[51] P. Ganesh and M. Widom, Phys. Rev. B **74**, 134205 (2006).
[52] C. Z. Wang, C. T. Chan, and K. M. Ho, Phys. Rev. B **45**, 12227 (1992).
[53] S. Plimpton, J. Comput. Phys. **117**, 1 (1995).